Far-Ultraviolet Number Counts of Field Galaxies

Elysse N. Voyer[1]

Department of Physics, The Catholic University of America, Washington, D.C. 20064

48voyer@cardinalmail.cua.edu

Jonathan P. Gardner

Astrophysics Science Division, Observational Cosmology Laboratory, Goddard Space Flight Center, Code 665, Greenbelt, MD 20771

Harry I. Teplitz

Spitzer Science Center, California Institute of Technology, 220-6, Pasadena, CA 91125

Brian D. Siana

California Institute of Technology, MS 105-24, Pasadena, CA 91125

and

Duilia F. de Mello

Department of Physics, The Catholic University of America, Washington, D.C. 20064

Received _____; accepted _____

[1]NASA Graduate Student Research Program Fellow

ABSTRACT

The Number counts of far-ultraviolet (FUV) galaxies as a function of magnitude provide a direct statistical measure of the density and evolution of star-forming galaxies. We report on the results of measurements of the rest-frame FUV number counts computed from data of several fields including the Hubble Ultra Deep Field, the Hubble Deep Field North, and the GOODS-North and -South fields. These data were obtained from the Hubble Space Telescope Solar Blind Channel of the Advance Camera for Surveys. The number counts cover an AB magnitude range from 20-29 magnitudes, covering a total area of 15.9 arcmin^2. We show that the number counts are lower than those in previous studies using smaller areas. The differences in the counts are likely the result of cosmic variance; our new data cover more area and more lines of sight than the previous studies. The slope of our number counts connects well with local FUV counts and they show good agreement with recent semi-analytical models based on dark matter "merger trees".

Subject headings: cosmology:observations-galaxies:evolution-galaxies:statistics-ultraviolet:galaxies

1. Introduction

Constructing the number distribution of field galaxies within an observed area versus magnitude is one of the fundamental techniques used to study galaxy evolution throughout cosmic time. These galaxy number counts are used to test theoretical models of galaxy evolution; changes in the slope of number count distributions reflect physical changes in the underlying galaxy populations. Such models can predict galaxy properties in various bandpasses and for various redshifts (z). At observed ultraviolet (UV) wavelengths, galaxy counts probe unobscured star-formation at rest-frame far-UV (FUV) wavelengths for $z < 1$, after which the Lyman limit (912Å) shifts into the observed bandpass. For this reason, number counts of UV detected galaxies provide a window into extragalactic star-formation history.

The UV cut-off of earth's atmosphere makes rest-frame FUV number count studies only possible with space-based observations. Over the past two decades, only a handful of space-based field galaxy surveys have been carried out at UV wavelengths (Milliard et al. 1992; Deharveng et al. 1994; Gardner et al. 2000; Iglesias-Páramo et al. 2004; Xu et al. 2005; Teplitz et al. 2006; Hoversten et al. 2009) since long integration times are required to reach faint magnitudes. The first UV galaxy counts were measured by Milliard et al. (1992) using the balloon-borne FOCA instrument at 2000Å and bright magnitudes, covering a large area of sky ($\sim$6 deg^2). Later, faint NUV and FUV galaxy counts were measured over smaller areas with the Hubble Space Telescope (HST) by Gardner et al. (2000) in the Hubble Deep Fields North and South (HDF-N & -S) and by Teplitz et al. (2006) in the HDF-N, covering 1.54 and 3.77 arcmin^2 respectively. Bright galaxy counts were measured using the Galaxy Evolution Explorer (GALEX) in larger fields ($\sim$20 deg^2) by Xu et al. (2005). More recently, Hoversten et al. (2009) used the *Swift* UV/Optical Telescope to measure NUV galaxy counts in a 289 arcmin^2 area of the Chandra Deep Field South (CDF-S). However,

the only two studies measuring the faint end slope of the FUV galaxy counts are biased by cosmic variance effects, due to the small areas surveyed, and known overdensities in the HDF-N (Cohen et al. 2000).

In this paper we present faint FUV (1500Å) galaxy number counts from deep images obtained with HSTs Solar Blind Channel (SBC) on the Advanced Camera for Surveys (ACS). These observations sample the largest area ever covered at these wavelengths (15.9 arcmin^2), just over four times the size of previous faint FUV number count studies. In Section 2 we present the data used for this study. In Section 3.1 we discuss the measurement of the number counts and corrections to the counts due to observational biases. The number counts are compared with previous studies and theoretical models in Section 3.2. Cosmic variance is discussed in Section 3.3, and the FUV extragalactic background light (EBL) calculation is presented in Section 3.4. Results of this study are summarized in Section 4.

2. The Data

For this study we used FUV observations from three different data sets: the HDF-N area of the Great Observatories Origins Deep Survey North (GOODS-N) field, the Hubble Ultra Deep Field (HUDF) area of the GOODS-South (GOODS-S) field, and smaller fields in various parts of the GOODS-N and -S fields. The HDF-N data is from the HST General Observer Program 9478, the HUDF data is from the HST Cycle 13 Treasury Program 10403, and the smaller GOODS-N and -S fields are from the HST Cycle 15 General Observer Program 10872. All observations were obtained with the SBC detector on Hubble's ACS. The ACS SBC detector is a Multi-Anode Microchannel Array (MAMA) with a field of view of $34''.6 \times 30''.8$. All observations were taken through the long-pass quartz filter, F150LP, that peaks ~1500Å, has a bandwidth of ~550Å, and a FWHM=177Å.

Final images of the HDF-N and HUDF used for source detection were constructed using the DRIZZLE package in IRAF[1]. The smaller GOODS-N and -S images were tiled onto the original GOODS areas for source detection. All reduction and photometry procedures for these data are described by Teplitz et al. (2010). We detected 113 FUV sources in the HUDF area of GOODS-S, 118 FUV sources in the smaller GOODS-N and -S images, and 100 FUV sources from the HDF-N area of GOODS-N. We removed 14 sources because they were too close to the edges of the images, leaving 317 sources to be included in the measurement of the number counts. The total catalog covers an AB magnitude range from 20-29 and their magnitude limit is ~28.5 as shown by the magnitude distribution in Figure 1. Photometric redshifts (z_{phot}) were available for 149 sources (Dahlen et al. 2007) and the distribution is shown in Figure 2. They are compared to spectroscopic redshifts (z_{spec}) where available in Figure 3 (Cohen 2001; Dawson et al. 2001).

3. Number Counts in the FUV

3.1. Measurement of Number Counts

In order to measure the number counts of galaxies in our sample we used the method in Gardner et al. (2000). Both the AB magnitude and size of a galaxy are required to calculate the total area over which a galaxy would be detected. FUV AB magnitudes (FUV_{AB}) of sources in all observed fields were obtained from catalogs produced with the SExtractor software package (Bertin & Arnouts 1996). Details on the production of these catalogs can be found in Teplitz et al. (2010). Sizes of these sources are determined from SEXtractor

[1]IRAF is distributed by the National Optical Astronomy Observatories, which is operated by the Association of Universities for Research in Astronomy, Inc., under cooperative agreement with the National Science Foundation.

optical $V + I$ segmentation maps created using 3.25σ isophotes on optical sources. These same isophotes were used to do the FUV photometry on the SBC images in Teplitz et al. (2010). From this information, we calculate, for each source, the maximum error in a pixel at 3σ as the flux of the source over three times the square-root of the source size. The pixels with errors less than or equal to this value make up the total area over which the source would be detected at 3σ. We detect this area in root-mean-square (RMS) error maps that we produce from the weight maps of the drizzled SBC images with the IRAF program *imcalc*. Small-scale-variations introduced into the images during drizzling are smoothed in the RMS maps with a $0''.4 \times 0''.4$ median filter.

We remove 14 sources from the number counts because they lie on the edges of the FUV images causing their areas to be partially cut-off. In order to be consistent, and not overestimate the detection area of the other sources, we cut down the edges of each RMS map by a length equal to the radius of the circular area of each source before calculating their detection areas. This includes both the outer edges of images, as well as edges on the inner parts of the images where drizzled fields do not overlap in the HUDF and HDF-N.

To correct for incompleteness in each magnitude bin of the number counts we use a method of bootstrap-sampling the size distribution of the version 2.0 GOODS-S V-band catalog[2] starting with a randomly generated FUV galaxy sample. First, the FUV magnitudes of the random sample are generated using the *RANDOMU* function in Interactive Data Language (IDL). We generate 1000 galaxies for each FUV magnitude bin. Next, we use the mean and standard deviation parameters of a Gaussian distribution fit to the FUV-V color distribution in the HUDF between $24 \leqslant m_{AB} \leqslant 28$ to randomly generate FUV-V colors using the *RANDOMN* function in IDL. This range is selected because the magnitude limit of the FUV catalog is ~28.5 and there are very few galaxies in

[2]http://archive.stsci.edu/prepds/goods/

the HUDF with magnitudes < 24. Because the Gaussian color distribution does not vary greatly between the different SBC fields we only sample the HUDF. With these random FUV magnitudes and FUV-V colors we calculate the optical magnitudes of the randomly generated sample and match them to the closest optical magnitudes of sources in the GOODS-S V-band catalog. The sizes of these objects are then sampled from 3.25σ isophote segmentation maps produced from public GOODS V-band images with SExtractor. From the sizes and FUV magnitudes of the random sample we then calculate the maximum error value below which each simulated object would be detected, and proceed to calculate the total detection area for each simulated object in the SBC RMS maps. Finally, to get the completeness correction factor for each magnitude bin, we average per magnitude bin the detection areas of the simulated objects (including galaxies with zero detection area), and take the ratio with the average detection area of all real FUV sources in corresponding bins. We apply these correction factors to the measured FUV counts.

3.2. Comparison with Previous FUV Number Counts and Models

In Figure 4 we present the FUV number counts from this work along with their measured values in Table 1. Small number Poisson statistical errors are calculated for each point from Gehrels (1986) at the 1σ level. The circles represent our counts. The upside-down triangles represent counts done with SBC images of the HDF-N from Teplitz et al. (2006). The asterisks represent counts done with HST STIS in the HDF-N and HDF-S from Gardner et al. (2000). The squares represent counts done with the Galaxy Evolution Explorer (GALEX) from Xu et al. (2005) (hereafter XU05 field), and the upright triangles represent counts done with GALEX from Hammer et al. (2010) (hereafter HAM10 field). No color corrections are made between the SBC filter which peaks at 1500Å and the STIS and GALEX filters that have FUV central wavelengths at 1595Å and 1530Å respectively.

Our galaxy sample probes the faint end of the FUV number counts, with the majority of sources occupying magnitude bins 23.5-28.5. This is reflected in the error bars of these plotted points. The two faintest objects in our sample are located in the smaller GOODS-S fields and have $FUV_{AB} = 29.04$ and 29.09. We binned these objects by 1/4 magnitude, with the bin centered at 29.125, to take into account the sharp drop-off in survey sensitivity at $FUV_{AB} > 29$. On average our number counts are ~30% lower than the faint FUV counts from Gardner et al. (2000) and Teplitz et al. (2006). The greatest differences are with the HDF-N SBC counts at the bright end and the HDF-N STIS count in the 29^{th} magnitude bin. In the central magnitude bins these counts are relatively consistent. The differences in the measurements are likely the result of cosmic variance which is discussed in more detail in Section 3.3.

At the 22.5 magnitude bin the slope of our number counts connects better with the faint end of the GALEX HAM10 field counts than with the XU05 field. It is not well understood why the GALEX counts diverge from each other after FUV_{AB} ~21.25, but Hammer et al. (2010) show the divergence can not be due to their source detection/photometry methods, AGN, or cosmic variance between fields. Also, while cluster members in the HAM10 field bias the bright bins of these number counts, they only compose ~2% of objects in the faintest bin, which represents the limiting depth of the survey.

Two of the primary uses of galaxy number counts are to test and constrain models of galaxy evolution. In Figure 4 we compare our FUV number counts with four different models. The 'fiducial', 'low', and WMAP5 models are the latest ΛCDM semi-analytical models based on dark matter "merger trees" from Gilmore et al. (2009). These models are characterized by both cosmological parameters and galaxy formation parameters that include: photoionization squelching, quiescent star formation, burst star formation, merger remnants and morphology, supernovae feedback, chemical evolution, black-hole growth,

AGN-driven winds, and radio-mode feedback (Somerville et al. 2008). The only galaxy formation parameters that change between these models are (1) star-formation efficiency, (2) radio mode heating, and (3) scattering parameters. The fourth model we use for comparison is the SB4/Lyα-flat SED model from Xu et al. (2005), that is characterized by a UV luminosity evolution, $L^* \sim (1+ z)^{2.5}$ and has the same UV spectral-energy distribution as a no-evolution model, except for a flat spectrum between 1200Å and 1000Å. This model is lower than the three semi-analytical models up to FUV_{AB} ~25, when all four models coincide, and then continues to match the 'fiducial' and WMAP5 models to faint magnitudes. The differences in the bright end of the models may be due to the fact that the SB4/Lyα-flat SED model is derived from a single spectral-energy distribution (Starburst 4 from Kinney et al. (1996)).

Our observed number counts are in good agreement with the ΛCDM semi-analytical models over all FUV magnitudes, perhaps with a slight preference for the WMAP5 model. The differences in the slopes of the models are caused by the different primordial power spectrum parameters (σ_8) that depends on the cosmology of the model used, or the number of low luminosity galaxies applied in the model. It is not obvious which of these are reflected in the slope of the observed number counts because these parameters can be degenerate between models. For instance, the 'low' model and the 'fiducial' model are derived from different cosmologies (concordance cosmology with parameters Ω_m=0.3, Ω_Λ=0.7, h=0.70, σ_8=0.90, and a WMAP3 cosmology with parameters Ω_m=0.2383, Ω_Λ=0.7617, h = 0.732, σ_8=0.761, respectively), but the 'low' model also has fewer low luminosity galaxies. Either, or both of these effects could contribute to the reduction in the faint end of the 'low' model as compared to the 'fiducial' model. The only cosmological difference between the 'low' model and the WMAP5 model is the value of the primordial power spectrum which is σ_8=0.82 for WMAP5. However, the WMAP5 model also overproduces bright galaxies compared to GALEX data. Previous FUV number counts do not consistently follow any of

these three semi-analytical models. Both sets of GALEX counts are lower than the models at the bright end, however the HAM10 field counts start to coincide with the models at FUV_{AB} >22.5. When plotting the SB4/Lyα-flat SED model we did not color correct the model from the GALEX FUV central wavelength at 1530Å to the SBC central wavelength at 1500Å. Our number counts do not consistently match this model, but coincide with it only at the magnitudes where it converges with the semi-analytical models at 25.5 and 28.5. As discussed by Teplitz et al. (2006) and Hammer et al. (2010), the discrepancies with this model, especially towards bright magnitudes, may suggest a need for number density evolution in FUV galaxy number count models.

3.3. Effects of Cosmic Variance

Uncertainties in measurements of galaxy number counts can arise as a result of clustering variations in an observed field due to the overall large-scale structure, or cosmic variance. The observations used for this study were designed to significantly reduce the effects of cosmic variance by including data from various sight-lines and covering a larger area than any previous FUV number counts study. Our observations cover a total area of 15.9 arcmin^2, while the Gardner et al. (2000) STIS observations in the HDF-N and -S cover only 1.54 arcmin^2 and the Teplitz et al. (2006) SBC observations in the HDF-N cover only ~3.77 arcmin^2. Also, the HDF-N has galaxy overdensities at z ~0.45 and z ~0.8 (Cohen et al. 2000) that bias the number counts in that field. To demonstrate the effects of cosmic variance we have plotted, in Figure 5, our total FUV number counts along with the number counts calculated for each SBC field individually. The circles represent the total number counts, the asterisks are counts in the HUDF area of GOODS-S, the upside down triangles are counts in the HDF-N area of GOODS-N, the squares are counts in the 6 smaller (< 1 arcmin^2) deep fields at various pointings in GOODS-N, and the triangles are counts in the

9 smaller deep fields at various pointings in GOODS-S. The HDF-N area counts are higher than the total counts, except at $FUV_{AB} = 28.5$, and in most cases also higher than counts in any other field. This suggests that previous FUV number counts results have been biased by the small field of view and overdensities in the HDF-N. The counts in the HUDF area are nearly the same or lower than the total counts, except for the 21.5 and 22.5 magnitude bins. This is most likely because the HUDF has the largest area of all the individual fields. We do not do a comparison in the two brightest magnitude bins (20.5 and 21.5) and the faintest magnitude bin (29.5) because there are too few objects in these bins, due to low signal-to-noise, to make a meaningful comparison.

3.4. The Extragalactic Background Light from Resolved Sources

The resolved FUV extragalactic background light (EBL) is a measure of the total integrated flux emitted from FUV detected galaxies and essentially quantifies the on-going star-formation in the universe. This value sets a lower limit for the diffuse (or total) EBL that also includes FUV light scattered isotropically by dust, HII two-photon emission, hot gas line emission, QSOs, AGNs, and the intergalactic medium (Bowyer 1991), theoretically providing an overall gauge of star-formation throughout cosmic time. The diffuse light was measured at FUV wavelengths (1450-1900Å) by Brown et al. (2000) using HST Space Telescope Imaging Spectrograph (STIS) observations of the HDF-N and -S and HDF-N parallel imaging. They used a mask to remove the optically detected objects down to m_{AB} = 29 from their images and found there is an unresolved component. They measured a diffuse FUV EBL of 501 ± 103 photons cm^{-2} s^{-1} sr^{-1} $Å^{-1}$. This is higher than the FUV EBL measured by initial studies (see review by Bowyer (1991)) of ~300 photons cm^{-2} s^{-1} sr^{-1} $Å^{-1}$.

We have calculated the FUV extragalactic background light (EBL) from the resolved

sources in our data. We use both sets of bright GALEX number counts in our calculation, giving us two possible values for the integrated EBL. First, we fit a slope of 0.23 ± 0.03 with an intercept of -1.88 ± 0.89 to our FUV number counts, and slope of 0.53 ± 0.01 with an intercept of -9.11 ± 0.28 to the XU05 GALEX counts. For the HAM10 field GALEX counts we use the slope of 0.5 fitted to the FUV data by Hammer et al. (2010) with an intercept of -8.7 ± 0.81. Next, these slopes, as well as the number counts, are converted to units of EBL per magnitude bin, erg s^{-1} cm^2 Hz^{-1} sr^{-1}, using the formula from Madau & Pozzetti (2000):

$$I_\nu = 10^{-0.4(FUV_{AB}+48.6)} N(FUV_{AB}) \quad (1)$$

This is plotted in Figure 6. Finally, we integrate under each function. For the combined fit with the XU05 data we set (hereafter EBL I) FUV_{AB} = 24.45 as the upper limit for the integral of the XU05 function and the lower limit for the integral of the SBC/FUV function, because this magnitude is the maximum in integrated light. From this model we measure the integrated EBL for the magnitude range FUV_{AB} = 14–30 of $\nu I_\nu = 1.4^{+0.2}_{-0.2}$ nW m^{-2} sr^{-1}, or in photon units, $I_\lambda = 71.4^{+10.4}_{-9.8}$ photons s^{-1} cm^{-2} sr^{-1} $Å^{-1}$. For the combined fit with the HAM10 data (hereafter EBL II) we set FUV_{AB} = 23.9 as the upper limit for the integral of the HAM10 function and the lower limit for the integral of the SBC/FUV function. From this model we measure the integrated EBL for the magnitude range FUV_{AB} = 17–30 of $\nu I_\nu = 1.7^{+0.4}_{-0.3}$ nW m^{-2} sr^{-1}, or in photon units, $I_\lambda = 88.0^{+18.1}_{-15.2}$ photons s^{-1} cm^{-2} sr^{-1} $Å^{-1}$. The errors are from the Poisonnian 1σ uncertainties on the number counts. Our measurements for EBL I and EBL II are ~52–64% and ~41–56% lower, respectively, than that from Gardner et al. (2000) who measured a range of $2.9^{+0.6}_{-0.4}$–$3.9^{+1.1}_{-0.8}$ nW m^{-2} sr^{-1} (144^{+28}_{-19}–195^{+59}_{-39} photons s^{-1} cm^{-2} sr^{-1} $Å^{-1}$). Xu et al. (2005) extrapolated models fit to the GALEX number counts, integrated these functions to zero flux, and measured the total FUV EBL to be 1.03 ± 0.15 nW m^{-2} sr^{-1} which is ~26% lower than EBL I, ~39% lower than EBL II, and also below the Gardner et al. (2000) range. The UV EBL was measured

at 2000Å by Milliard et al. (1992) from FOCA number counts and by Armand et al. (1994) from predictions of number counts (Armand & Milliard 1994). While our measurments are well within the range of 40–130 photons s^{-1} cm^{-2} sr^{-1} $Å^{-1}$ predicted by Armand et al. (1994), they are much higher than the 23 photons s^{-1} cm^{-2} sr^{-1} $Å^{-1}$ determined from the FOCA number counts. All values for the resolved and diffuse FUV EBL discussed here are summarized in Table 2.

4. Summary

We have presented FUV galaxy number counts at 1500Å measured from deep HST ACS/SBC observations of the HUDF area of the GOODS-S field, the HDF-N area of the GOODS-N field, and 15 smaller fields at various pointings in GOODS-N and -S. We sample the faint end of the FUV number counts out to FUV_{AB} ~29 with the majority of the sources in magnitude bins 23.5-28.5 and cover a larger area (15.9 $arcmin^2$) then previously observed at these wavelength and magnitude ranges. The number counts distribution provides the following results:

1. A power law slope of 0.23 ± 0.03 (intercept of -1.88 ± 0.89) fits the shape of the logarithmic number counts distribution for FUV_{AB} magnitudes from 20.5 to 29.125.

2. These number counts are 30% lower than what has been found from previous measurements of FUV number counts that were measured only in the HDF-N area of the GOODS-N field. This difference is most likely due to cosmic variance because the HDF-N samples a small area and there are known overdensities in this field, and these new FUV data sample more area and sight-lines than ever before. The cosmic variance between fields is evident when number counts are calculated in the individual SBC fields and compared to the total overall counts.

3. The bright end of the number counts slope, at $FUV_{AB} = 22.5$, connects well with the recent GALEX FUV number counts in the HAM10 field but is higher than the GALEX FUV counts in the XU05 field.

4. The number counts are in good agreement with the latest λCDM semi-analytical models based on concordance, WMAP3, and WMAP5 cosmologies, with a slight preference for the WMAP5 model. They only coincide with the SB4/Lyα-flat SED model at FUV_{AB} = 25.5 and 28.5 which is likely due to the fact that this model is based on a single starburst SED and offers evidence for number density evolution.

5. The integrated light from field galaxies contributes $1.4^{+0.2}_{-0.2}$ nW m^{-2} sr^{-1} or $71.4^{+10.4}_{-9.8}$ photons s^{-1} cm^{-2} sr^{-1} Å^{-1} to the FUV extragalactic background light for magnitudes 14-30 when measured with XU05 bright end GALEX counts, and $1.7^{+0.4}_{-0.3}$ nW m^{-2} sr^{-1} or $88.0^{+18.1}_{-15.2}$ photons s^{-1} cm^{-2} sr^{-1} Å^{-1} for magnitudes 17-30 when measured with HAM10 bright end GALEX counts. These measurements show that the integrated FUV light from resolved objects makes up ~14–17% of the diffuse (or total) extragalactic background light which was most recently measured as 501 photons s^{-1} cm^{-2} sr^{-1} Å^{-1} (Brown et al. 2000). This measurement sets a lower limit for future calculations of the diffuse background.

We would like to thank Rudy Gilmore and Kevin Xu for providing us with theoretical number counts models, Rachel Somerville for helpful discussion of semi-analytical models and commenting on Section 3.2 of this paper, and Derek Hammer for helpful science discussions and sharing number counts results. Support for this research was provided by HST GO-10403, GO-###, and GO-###. E.N.V. was funded by the NASA Graduate Research Program grant #NNX08AR95H.

REFERENCES

Armand, C., & Milliard, B. 1994, A&A, 282, 1

Armand, C., Milliard, B., & Deharveng, J. M. 1994, A&A, 284, 12

Bertin, E., & Arnouts, S. 1996, A&AS, 117, 393

Bowyer, S. 1991, ARA&A, 29, 59

Brown, T. M., Kimble, R. A., Ferguson, H. C., Gardner, J. P., Collins, N. R., & Hill, R. S. 2000, AJ, 120, 1153

Cohen, J. G., Hogg, D. W., Blandford, R., Cowie, L. L., Hu, E., Songaila, A., Shopbell, P., & Richberg, K. 2000, ApJ, 538, 29

Cohen, J. G. 2001, AJ, 121, 2895

Dahlen, T., Mobasher, B., Dickinson, M., Ferguson, H. C., Giavalisco, M., Kretchmer, C., & Ravindranath, S. 2007, ApJ, 654, 172

Dawson, S., Stern, D., Bunker, A. J., Spinrad, H., & Dey, A. 2001, AJ, 122, 598

de Mello, D. F., Gardner, J. P., Dahlen, T., Conselice, C. J., Grogin, N. A., & Koekemoer, A. M. 2004, ApJ, 600, L151

Deharveng, J.-M., Sasseen, T. P., Buat, V., Bowyer, S., Lampton, M., & Wu, X. 1994, A&A, 289, 715

Gardner, J. P., Brown, T. M., & Ferguson, H. C. 2000, ApJ, 542, L79

Gehrels, N. 1986, ApJ, 303, 336

Gilmore, R. C., Madau, P., Primack, J. R., Somerville, R. S., & Haardt, F. 2009, MNRAS, 399, 1694

Hammer, D., Hornschemeier, A., Mobasher, B., Miller, N., Smith, R., Arnouts, S., Milliard, B., & Jenkins, L. 2010, arXiv:1004.2498

Hoversten, E. A., et al. 2009, ApJ, 705, 1462

Iglesias-Páramo, J., Buat, V., Donas, J., Boselli, A., & Milliard, B. 2004, A&A, 419, 109

Kinney, A. L., Calzetti, D., Bohlin, R. C., McQuade, K., Storchi-Bergmann, T., & Schmitt, H. R. 1996, ApJ, 467, 38

Madau, P., & Pozzetti, L. 2000, MNRAS, 312, L9

Milliard, B., Donas, J., Laget, M., Armand, C., & Vuillemin, A. 1992, A&A, 257, 24

Somerville, R. S., Hopkins, P. F., Cox, T. J., Robertson, B. E., & Hernquist, L. 2008, MNRAS, 391, 481

Teplitz, H. I., et al. 2006, AJ, 132, 853

Teplitz, H. I., et al. 2010, in preparation

Xu, C. K., et al. 2005, ApJ, 619, L11

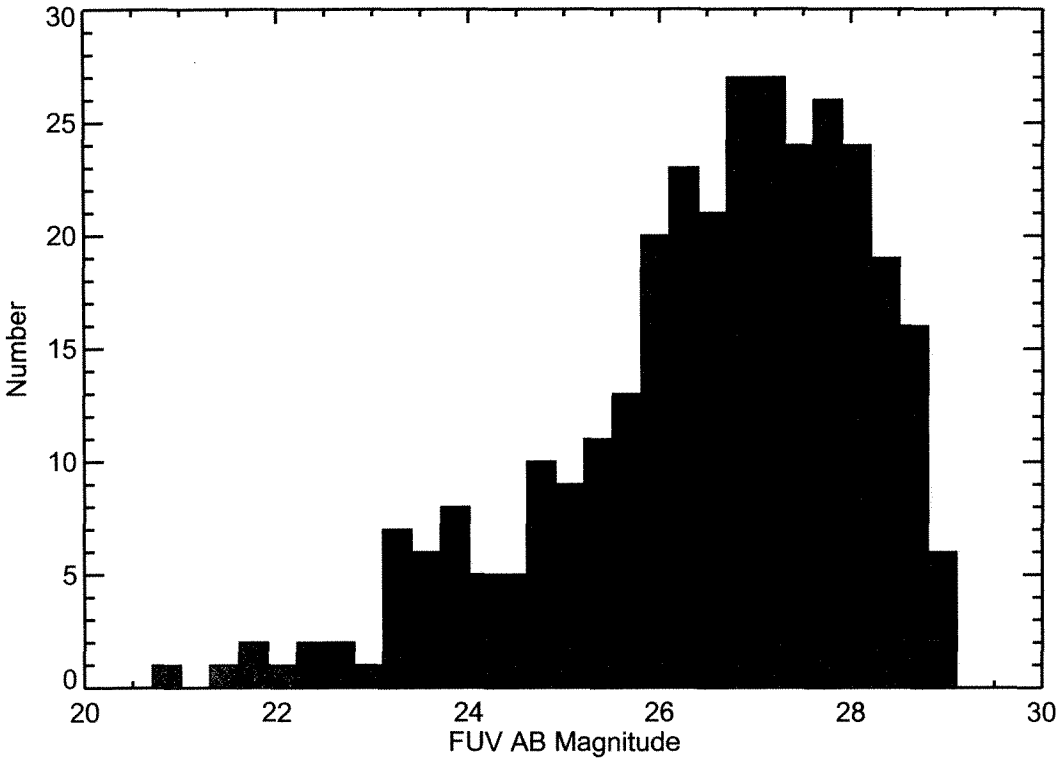

Fig. 1.— FUV magnitude distribution for all 317 sources used to measure FUV number counts.

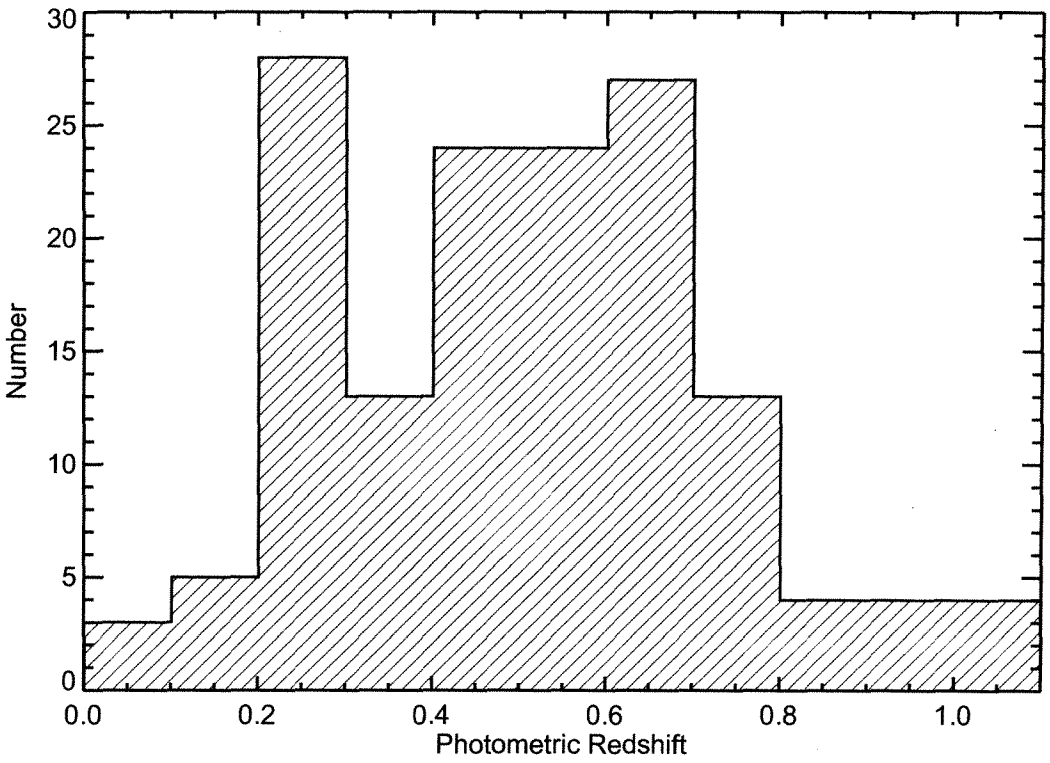

Fig. 2.— Distribution of photometric redshifts, where available, for 149 sources from FUV number counts. Redshifts are from the GOODS catalog (Dahlen et al. 2007).

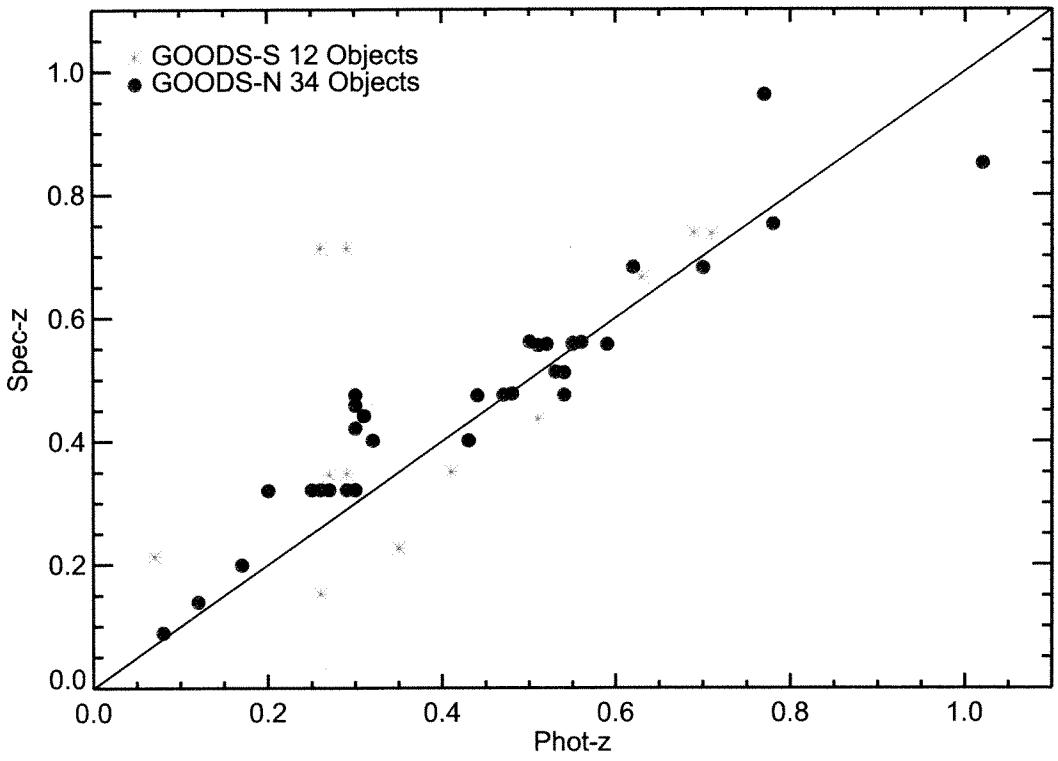

Fig. 3.— Spectroscopic redshifts versus photometric redshifts for FUV sources, where available (Cohen 2001; Dawson et al. 2001).

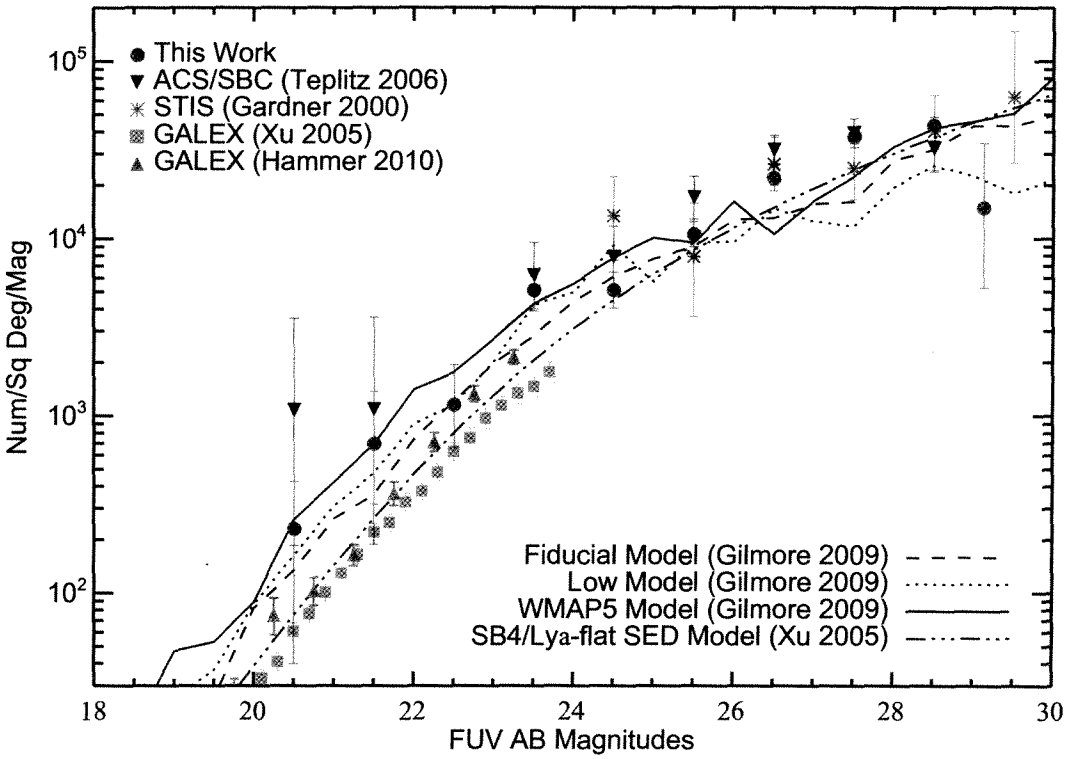

Fig. 4.— FUV number counts of field galaxies from this work shown with FUV number counts from previous studies and compared to semi-analytical models. Error bars are Poissonnian from Gehrels (1986). At $m_{AB} > 29$, 0.25 magnitude bins were used to accommodate the sharp drop-off in survey sensitivity over most the area.

Table 1. FUV Galaxy Counts

FUV_{AB} (mag)	NC (No. deg^{-2} mag^{-1})	log NC	σ_{low}	σ_{high}	Raw No.
20.5	230	2.36	0.76	0.26	1
21.5	694	2.84	0.34	0.29	3
22.5	1157	3.06	0.24	0.22	5
23.5	5114	3.70	0.10	0.10	22
24.5	5119	3.70	0.10	0.10	22
25.5	10567	4.02	0.07	0.07	44
26.5	21927	4.34	0.04	0.06	78
27.5	37527	4.57	0.03	0.06	88
28.5	43586	4.64	0.08	0.05	52
29.125	14926	4.17	0.45	0.36	2

Note—Magnitudes represent the center of the bins and errors are 1σ Poisonnian (Gehrels 1986). At AB>29, 0.25 magnitude bins are used to accommodate the sharp drop-off in survey sensitivity over most of the area.

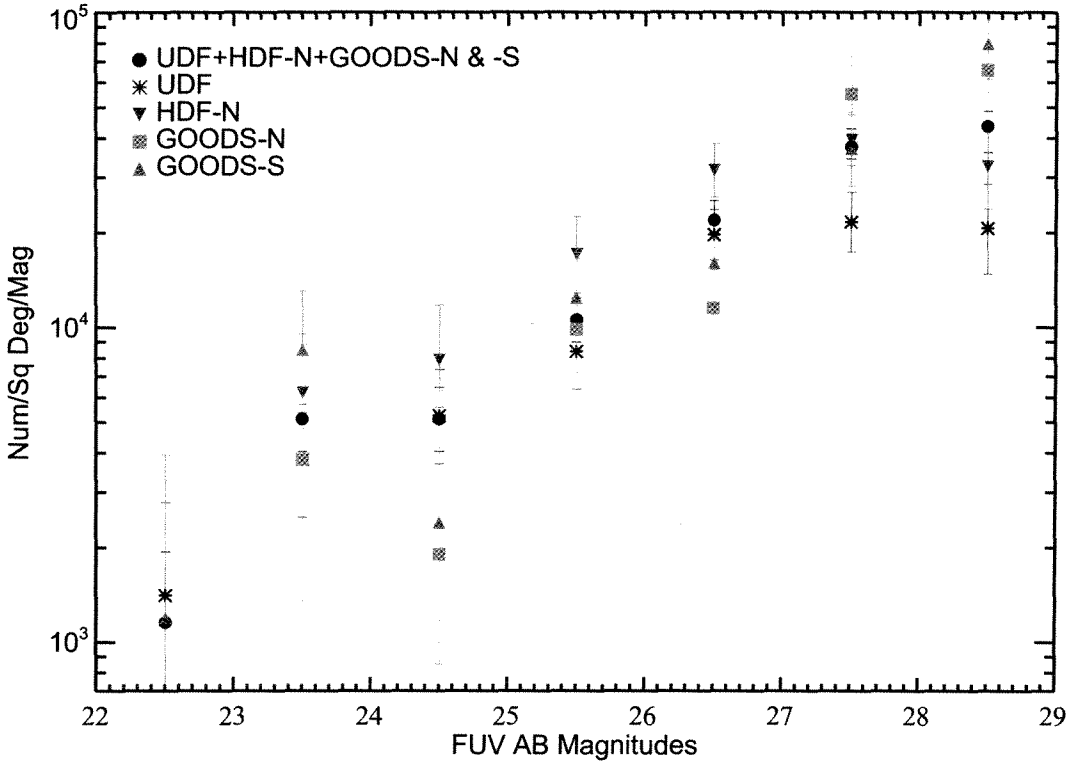

Fig. 5.— FUV number counts for individual fields. These illustrates the cosmic variance between fields. We excluded the two brightest (20.5 and 21.5 mag) and the faintest (29.5 mag) magnitude bins from this plot because there is not enough signal-to-noise to make a comparison between fields at these magnitudes. HDF-N counts are from Teplitz et al. (2006).

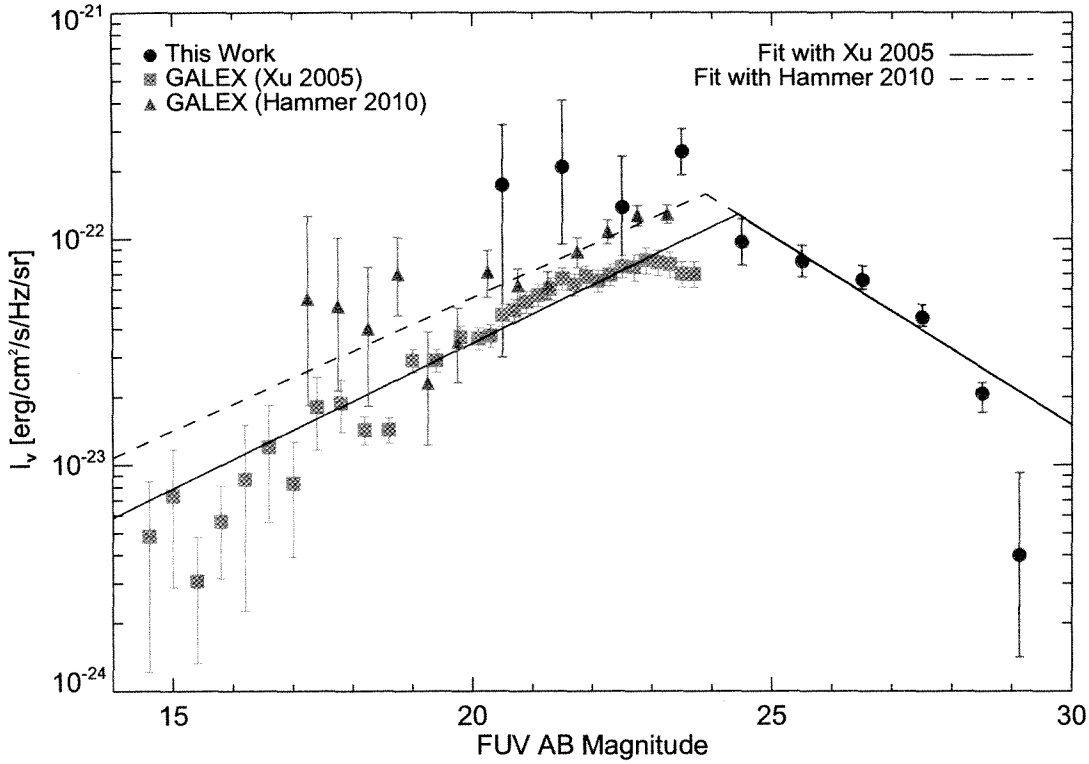

Fig. 6.— Extragalactic background light from resolved sources per magnitude as a function of FUV magnitude. Two measurements are made from these data. The solid line measures the integrated EBL using the XU05 counts for the bright end (EBL I), while the dashed line makes this measurement using the HAM10 counts at the bright end (EBL II).

Table 2. MEASUREMENTS OF THE FUV EXTRAGALACTIC BACKGROUND LIGHT

Investigators	Instrument	λ[a] (Å)	FUV EBL (nW m^{-2} sr^{-1})	FUV EBL (photons s^{-1} cm^{-2} sr^{-1} Å^{-1})
		Resolved Measurements		
This Work: EBL I[b]	SBC/GALEX	1500/1530	$1.4^{+0.2}_{-0.2}$	$71.4^{+10.4}_{-9.8}$
This Work: EBL II[c]	SBC/GALEX	1500/1530	$1.7^{+0.4}_{-0.3}$	$88.0^{+18.1}_{-15.2}$
Xu et al. (2005)	GALEX	1530	1.03 ± 0.15	52 ± 7
Gardner et al. (2000)	STIS/FOCA	1595	$2.9^{+0.6}_{-0.4}$ to $3.9^{+1.1}_{-0.8}$	144^{+28}_{-19} to 195^{+59}_{-39}
Armand et al. (1994)[d]	-	2000	0.8 to 2.6	40 to 130
Milliard et al. (1992)	FOCA	2000	0.4	23
		Diffuse Measurements		
Brown et al. (2000)	STIS	1595	9.9	501
Bowyer (1991)[e]	-	-	-	~300

[a]Central wavelength of the filter used.

[b]Bright end fit is from Xu et al. (2005) GALEX FUV number counts.

[c]Bright end fit is from Hammer et al. (2010) GALEX FUV number counts.

[d]Second column is blank because this measurement is from a prediction of number counts based on

galaxy evolution models and published galaxy SEDs.

[e]Middle three columns are blank because this measurement is the combined result from multiple studies done over a range of FUV wavelengths.